



# Natural polymers-enhanced double-network hydrogel as wearable flexible sensor with high mechanical strength and strain sensitivity

Zhijie Zhao<sup>a,1</sup>, Xiao Fan<sup>a,1</sup>, Shuoxuan Wang<sup>a,1</sup>, Xiaoning Jin<sup>a</sup>, Junjie Li<sup>b,c,\*</sup>, Yuping Wei<sup>a,c,\*</sup>, Yong Wang<sup>a,\*</sup>

<sup>a</sup> Department of Chemistry, School of Science, Tianjin University, Tianjin 300350, China

<sup>b</sup> School of Chemical Engineering and Technology, Tianjin University, Tianjin 300350, China

<sup>c</sup> Frontiers Science Center for Synthetic Biology and Key Laboratory of Systems Bioengineering (Ministry of Education), Tianjin University, Tianjin 300350, China

## ARTICLE INFO

### Article history:

Received 22 June 2022

Revised 22 September 2022

Accepted 7 October 2022

Available online 12 October 2022

### Keywords:

Conductive hydrogel

Double network

Gelatin

Dialdehyde  $\beta$ -cyclodextrin

Sensor

## ABSTRACT

Conductive hydrogels have shown great prospects as wearable flexible sensors. Nevertheless, it is still a challenge to construct hydrogel-based sensor with great mechanical strength and high strain sensitivity. Herein, an ion-conducting hydrogel was fabricated by introducing gelatin-dialdehyde  $\beta$ -cyclodextrin (Gel-DACD) into polyvinyl alcohol-borax (PVA-borax) hydrogel network. Natural Gel-DACD network acted as mechanical deformation force through non-covalent cross-linking to endow the polyvinyl alcohol-borax/gelatin-dialdehyde  $\beta$ -cyclodextrin hydrogel (PGBCDH) with excellent mechanical stress (1.35 MPa), stretchability (400%), toughness (1.84 MJ/m<sup>3</sup>) and great fatigue resistance (200% strain for 100 cycles). Surprisingly, PGBCDH displayed good conductivity of 0.31 S/m after adding DACD to hydrogel network. As sensor, it showed rapid response (168 ms), high strain sensitivity (gage factor (GF)=8.57 in the strain range of 200%-250%) and reliable sensing stability (100% strain for 200 cycles). Importantly, PGBCDH-based sensor can accurately monitor complex body movements (knee, elbow, wrist and finger joints) and large-scale subtle movements (speech, swallow, breath and facial expressions). Thus, PGBCDH shows great potential for human monitoring with high precision.

© 2023 Published by Elsevier B.V. on behalf of Chinese Chemical Society and Institute of Materia Medica, Chinese Academy of Medical Sciences.

Electronic equipment with flexibility and portability have provoked extensive research in the domains of artificial intelligence, intelligent actuators and human-computer interactive systems [1–4]. Among them, conductive hydrogel as strain sensor installed on human body or clothing can convert diverse body movements and physiological information into electrical signals for actualizing accurate perception acquisition [5–7]. Typically, the conductive fillers (e.g., MXene, graphene, liquid metal and polypyrrole) are often introduced for fabricating electron-conducting hydrogel network [8–12]. However, conductive hydrogels obtained usually exhibit unstable conductivity and restricted mechanical performance due to the poor dispersion and low compatibility of stiff conductive fillers, blocking the reliability of human body data transmission and information communion [13,14]. Consequently, it is necessary to develop conductive hydrogels with great compatibility to insure its functionality of sensing devices.

In this respect, ion-conducting hydrogel is considered as ideal candidate since free ions can be uniformly dispersed and large amounts of water bound to hydrogel make them transport conveniently [15–17]. However, it keeps a challenge to balance the great electrical conductivity and excellent mechanical performance for ion-conducting hydrogel. Double-network (DN) hydrogels can enhance the mechanical strength, where the covalently associative network imparts structural integrity to hydrogel and the non-covalently associative network acts as mechanical deformation forces to offer high-energy strain output [18–20]. As previously reported, Yang *et al.* [21] fabricated a wearable flexible strain sensor based on lithium chloride (LiCl)/agar/polyacrylamide ionic hydrogel, but it exhibited relatively low tensile stress (220 kPa) and gage factor (GF) of 1.8 at large strain. Ding *et al.* [22] prepared a semi-interpenetrating network ionic composite using carboxymethyl chitosan/polyacrylamide/sodium chloride (NaCl) hydrogel with conductivity up to 6.44 S/m, yet it displayed breaking stress of 560 kPa and the GF of 0.214 corresponding to 300%–800% strain. However, the DN ion-conducting hydrogels exhibited low tensile stress and strain sensitivity and they can not perform sensing functions well. Gelatin (Gel) is a natural polymer derived from collagen,

\* Corresponding authors.

E-mail addresses: [li41308@tju.edu.cn](mailto:li41308@tju.edu.cn) (J. Li), [ypwei@tju.edu.cn](mailto:ypwei@tju.edu.cn) (Y. Wei), [wangyongtju@tju.edu.cn](mailto:wangyongtju@tju.edu.cn) (Y. Wang).

<sup>1</sup> These authors contributed equally to this work.

which can form triple helical structure to strengthen the hydrogel after its aqueous solution has cooled [23,24].  $\beta$ -cyclodextrin ( $\beta$ -CD) is a cyclic macromolecular oligosaccharide with hydroxyl group (-OH) at the edge of its cavity, which is easily functionalized by introducing new groups [25,26]. Additionally, polyvinyl alcohol (PVA) has desirable flexibility, outstanding elasticity, controllable molecular structures and selective chemical reactivity, making it an ideal substrate for reinforcing the mechanical properties of hydrogels [27,28]. Based on the double-network strategy, the gelatin-dialdehyde  $\beta$ -cyclodextrin (Gel-DACD) with increased physical cross-linking as first network via Schiff bonds between Gel and  $\beta$ -CD offer high-energy deformation output, and PVA with enhanced chemical cross-linking as second network maintain solid integrity. It is expected that the combination of Gel,  $\beta$ -CD and PVA may be an effective method to prepare the hydrogel of high tensile stress with good strain sensitivity and sensing stability as flexible strain sensor.

In our work, a conductive hydrogel was prepared by introducing natural gelatin-dialdehyde  $\beta$ -cyclodextrin (Gel-DACD) into synthetic PVA-borax hydrogel network via one-pot method. Gel-DACD network acted as sacrificial force through physical cross-linking to endow the polyvinyl alcohol-borax/gelatin-dialdehyde  $\beta$ -cyclodextrin hydrogel (PGBCDH) with excellent tensile strength (1.35 MPa), stretchability (400%), toughness (1.84 MJ/m<sup>3</sup>) and great fatigue resistance (200% strain for 100 cycles). Significantly, PGBCDH displayed good conductivity of 0.31 S/m after adding DACD to hydrogel network. As sensor, it displayed rapid response (168 ms), high strain sensitivity (GF=8.57 in the strain range of 200%–250%) and reliable sensing stability (100% strain for 200 cycles). Importantly, PGBCDH-based sensor can accurately monitor complex body movements (knee, elbow, wrist and finger joints) and large-scale subtle movements (speech, swallow, breath and facial expressions). Thus, PGBCDH displays huge potential in the field of flexible electronic skins for human monitoring with high-precision.

The preparation process of the ion-conducting PGBCDH was shown in Fig. 1a. Firstly, PVA, borax, Gel and DACD were dispersed in NaCl solution and mixed well. The mixed solution was placed at 50 °C for 6 h to promote the cross-linking of DACD and Gel to form Schiff base bonds as well as the cross-linking of PVA and Borax to form borate bonds. Then, it was placed at 4 °C for 1 h to stimulate the hydrogen bonds and triple helical structure of Gel chains to form spontaneously. Finally, the hydrogel was frozen and thawed between -18 °C and room temperature for ten times to promote the formation of PVA crystalline regions and intramolecular hydrogen bonding, as well as enhance the physical cross-linking between PVA and Gel chains. In the double network hydrogel system, natural Gel-DACD was recognized as the first polymer network structure and synthetic PVA-borax was selected as the second polymer network structure. Besides, Na<sup>+</sup> and Cl<sup>-</sup> were uniformly distributed inside the hydrogel, endowing the hydrogel excellent ionic conductivity.

PGBCDH can resist various twists, including tension, knotting, load bearing and compression (Fig. 1b). Specifically, PGBCDH was stretched to about 4 times its original length without breaking. And even a small knot on the hydrogel did not affect the stretchability. The excellent mechanical strength of PGBCDH was also reflected in the cylindrical hydrogel with a diameter of 8 mm that can easily withstand a weight of 3.25 kg without cracking. Moreover, PGBCDH also showed extremely strong compressive elasticity, which could quickly restore its original shape without any deformation once the compressive force released. These results showed that PGBCDH had excellent mechanical performance to adapt to the human movement as flexible strain sensor.

The FT-IR spectra of Borax, PVA, DACD, Gel and hydrogels composed of different components were shown in Figs. 2a and b. For PVA, the peaks appeared at 3433 cm<sup>-1</sup>, 2935–2905 cm<sup>-1</sup> and 1636 cm<sup>-1</sup> were assigned to -OH stretching vibration, -CH<sub>2</sub> stretching vibration and -OH bending vibration of absorb water, respectively. In PVA hydrogel (PH), the peak at 1156 cm<sup>-1</sup> was related to C-C

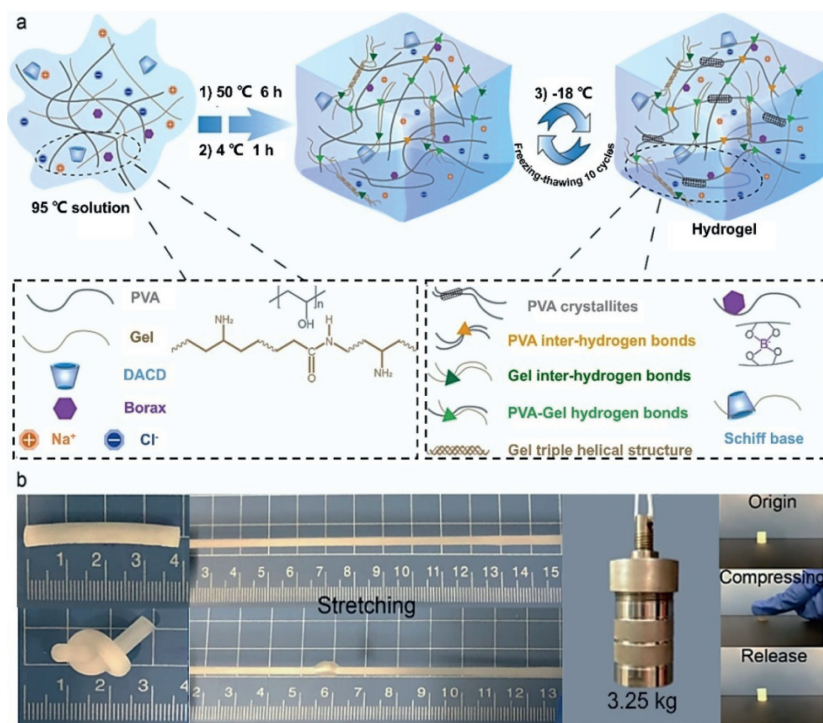


**Fig. 1.** (a) The schematic image of formation mechanism of PGBCDH. (b) Photographs of PGBCDH with outstanding mechanical properties to withstand stretching, knotting, load bearing and compression.

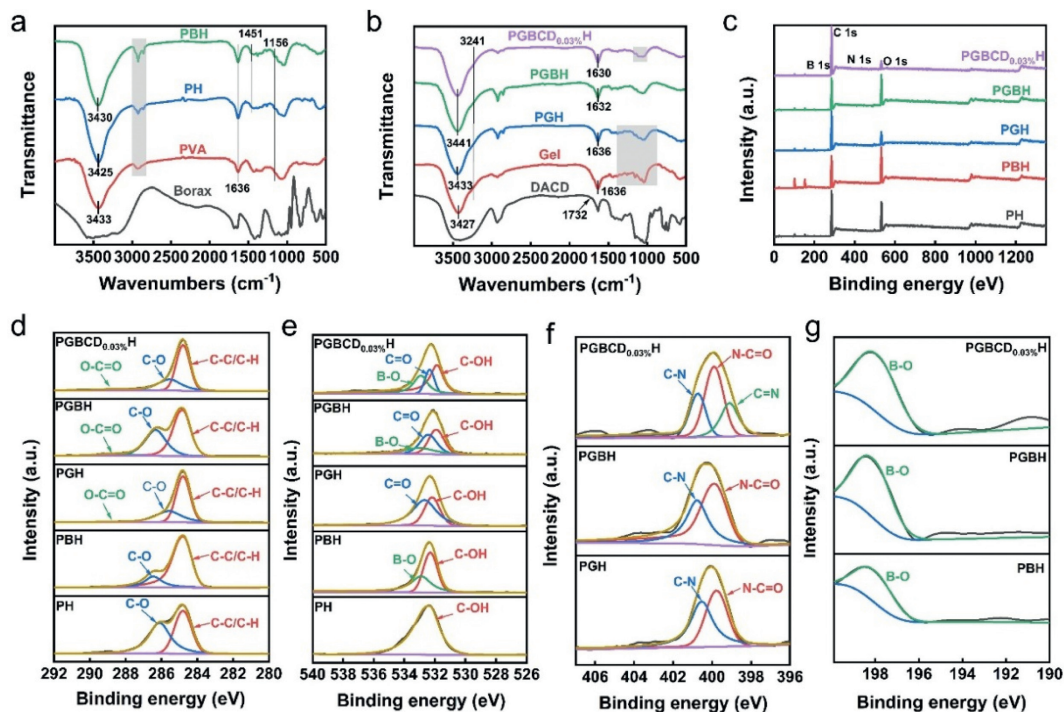


**Fig. 2.** IR spectra of (a) Borax, PVA, PH, and PBH; and (b) DACD, Gel, PGH, PGBH, and PGBCDH. XPS spectra of (c) PH, PBH, PGH, PGBH, and PGBCDH; (d) C 1s; (e) O 1s; (f) N 1s; and (g) B 1s.

stretching vibration, which was the symmetric stretching vibration peak of O–C–C (refer to the crystallinity phase of PVA); the peak at  $1101\text{ cm}^{-1}$  was assigned to C–O stretching vibration, which was the anti-symmetric stretching vibration peak of O–C–C (refer to the amorphous phase of PVA). Compared with PVA, the –OH stretching vibration shifted from  $3433\text{ cm}^{-1}$  to  $3425\text{ cm}^{-1}$  in PH, indicating that strong hydrogen bonding interactions occurred during freeze-thaw cycles. The characteristic peaks of borax were at  $625\text{ cm}^{-1}$  for B–O–B bending vibration and  $820\text{ cm}^{-1}$  for B–O stretching vibration. In PVA-borax hydrogel (PBH), the peaks at  $1451\text{ cm}^{-1}$  and  $1167\text{ cm}^{-1}$  were assigned to B–O–C asymmetric stretching relaxation and B–O–C stretching vibration, respectively. Compared with PVA, the peak at  $1091\text{ cm}^{-1}$  disappeared in PBH, suggesting the cross-linking between the borate ions and the PVA chains.

After the addition of borax, the peak of –OH stretching vibration in PBH shifted slightly from  $3425\text{ cm}^{-1}$  to  $3430\text{ cm}^{-1}$  due to the formation of borate ester bonds between hydroxyl and borate ions. For DACD, the peaks located at  $2926\text{ cm}^{-1}$ ,  $1030\text{ cm}^{-1}$  and  $1165\text{ cm}^{-1}$  referred to C–H stretching vibration, C–OH stretching vibration and C–O–C symmetric stretching vibration in  $\beta$ -CD, respectively. The peak appeared at  $1732\text{ cm}^{-1}$  was assigned as C=O stretching vibration, which proved that –OH of  $\beta$ -CD was efficiently oxidized to aldehyde group –CHO by  $\text{NaIO}_4$ . The peaks of Gel located at  $1638\text{ cm}^{-1}$  for amide I,  $1527\text{ cm}^{-1}$  for amide II and  $1233\text{ cm}^{-1}$  for amide III. In PVA/gelatin hydrogel (PGH), the peak at  $1200\text{--}800\text{ cm}^{-1}$  belonged to the typical C–C and C–O stretching vibration. In PVA-borax/gelatin hydrogel (PGBH), the peaks of  $3441$ ,  $2924$ ,  $1632$  and  $1514\text{ cm}^{-1}$  were attributed to –OH, C–H, C=O and C–N stretching vibrations, respectively. In PGBCDH, the peak at  $1000\text{--}1100\text{ cm}^{-1}$  was attributed to the reaction of –CHO of DACD with the hydroxyl group of PVA to form acetal group (O–C–O vibration).

The XPS spectra of PH, PBH, PGH, PGBH and PGBCDH were shown in Fig. 2c. The C 1s spectra of PH and PBH presented two carbon-related peaks, namely C–C/C–H and C–O (Fig. 2d). Compared with PH, the peak of C–O shifted from  $286.1\text{ eV}$  to  $286.5\text{ eV}$

in PBH owing to the formation of borate ester bonds. In addition, the peaks at  $288.7$ ,  $288.5$  and  $288.5\text{ eV}$  were related to O–C=O in PGH, PGBH and PGBCDH, respectively. The O–C=O peak moved from  $288.7\text{ eV}$  to  $288.5\text{ eV}$  in PGBH compared with PGH since the PVA-Gel hydrogen bonds were partially blocked by PVA-borax cross-linking network. In O 1s spectra of PBH, the peaks of C–OH at  $532.3\text{ eV}$  and B–O at  $532.9\text{ eV}$  were ascribed to the dynamic borate bonds formed through PVA and borax (Fig. 2e). The peaks at  $532.7\text{ eV}$ ,  $532.4\text{ eV}$  and  $532.3\text{ eV}$  were referred to C=O in PGH, PGBH and PGBCDH, respectively. Compared with PGH, the peak of C–O shifted from  $532.2\text{ eV}$  to  $531.9\text{ eV}$  in PGBH since the PVA inter-hydrogen bonds and PVA-Gel hydrogen bonds were weakened due to the increased cross-linking between the hydroxyl of PVA and borate ions. In N 1s spectrum of PGBCDH, the peaks at  $399.1\text{ eV}$ ,  $399.9\text{ eV}$  and  $400.7\text{ eV}$  are assigned to C=N, N–C=O and C–N, respectively, indicating the formation of the Schiff base bonds between DACD and Gel (Fig. 2f). In the spectra of B 1s, the peaks at  $198.0\text{ eV}$ ,  $198.1\text{ eV}$  and  $197.9\text{ eV}$  were assigned to B–O in PBH, PGBH and PGBCDH, respectively (Fig. 2g). Moreover, PGBCDH showed larger pore sizes than PGBH due to the increased degree of cross-linking and dense network structure as characterized by SEM analysis (Fig. S1 in Supporting information).

As shown in Fig. 3a, the tensile stress-strain curves were measured by mechanical tests. The fracture stress of PGBCDH was  $1.35\text{ MPa}$ , which was notably higher than PH ( $0.32\text{ MPa}$ ), PGH ( $0.72\text{ MPa}$ ), PBH ( $0.86\text{ MPa}$ ) and PGBH ( $1.11\text{ MPa}$ ) (Fig. 3b). And PGBCDH exhibited a good fracture strain of  $400\%$ , being better than PH of  $317\%$ , PGH of  $347\%$ , PBH of  $378\%$  and PGBH of  $349\%$ . Gelatin with tight triple-helix structure as well as the "salting-out" effect between gelatin and NaCl enhanced the mechanical properties of PGBCDH. The influence of DACD content on mechanical performance of hydrogels was investigated in Fig. 3c. With DACD content increasing from 0 to  $0.03\%$  w/v, the fracture stress and strain were enhanced since more DACD with abundant hydroxyl could offer increased mechanical deformation during stretching via the hydrogen bonds between Gel and DACD as sacrificial force

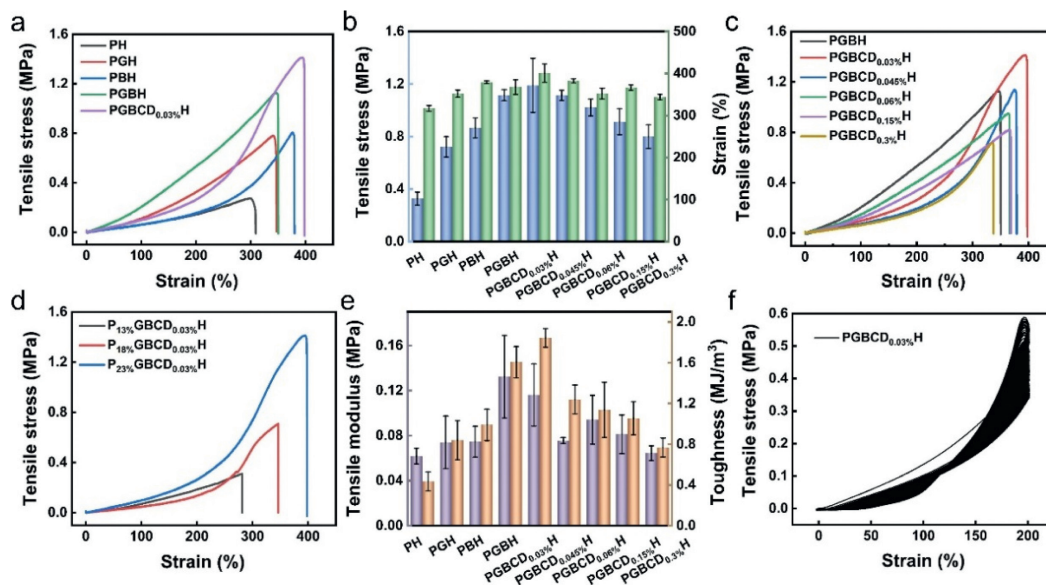


**Fig. 3.** (a-c) Typical tensile stress-strain curves of the hydrogels. (d) Tensile Stress and Strain values of the hydrogels. (e) Tensile modulus and toughness values of the hydrogels. (f) Cyclic tensile tests under 200% strain for 100 cycles.

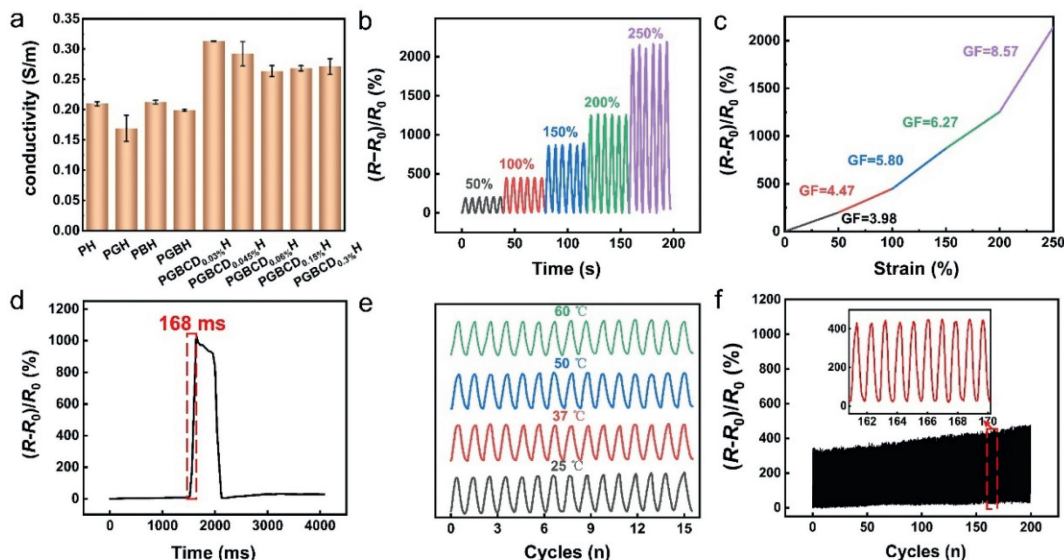


**Fig. 4.** (a) The ionic conductivity of hydrogels with different content. (b) Relative resistance changes of different repeated strains. (c) The increase of Gauge factor with the increase of tensile strain. (d) Response time of the hydrogel. (e) Stability of hydrogels at different temperatures. (f) Stability of the PGBCDH by applying repeated 100% strain for 200 cycles.

(Fig. 3b). While the DACD content increased from 0.03% to 0.3% w/v, the tensile stress and strain at break decreased to 0.75 MPa and 337%, respectively. It may be because excessive DACD hinder the partial formation of inter-crystalline entanglement of PVA chains and the triple-helical ordered structure in Gel [29]. Additionally, with the increase of PVA content, the fracture tensile stress and strain also increased since more PVA can form microdomain crosslinking sites to withstand tensile deformation (Fig. 3d). Synthetic PVA-borax network imparted structural integrity to hydrogel. PVA crystallites and rich intramolecular hydrogen bonds from PVA hydroxyl further gave PGBCDH good mechanical performance with both flexibility and strength. The elastic modulus of PH, PGH, PBH, PGBH and PGBCDH were 0.061, 0.072, 0.073, 0.131 and 0.115 MPa, respectively (Fig. 3e). In particular, the maximum toughness of PGBCDH can reach 1.84 MJ/m<sup>3</sup>, which was stronger than that of PBH (0.99 MJ/m<sup>3</sup>) and PGBH (1.60 MJ/m<sup>3</sup>). It

indicated that the introduction of Gel-DACD network made the hydrogel with more non-covalent and covalently cross-linked structures to resist mechanical strain than PBH and PGBH. The tensile reversibility of PGBCDH was recorded by cyclic tensile tests (Fig. 3f). PGBCDH did not exhibit a distinct hysteresis loop at 200% strain, indicating that dynamic cross-linked hydrogel can rapidly rebuild network structures to dissipate energy. The 100 consecutive loading-unloading tensile cycle tests also showed the excellent fatigue resistance of PGBCDH to repetitive deformation.

Conductivity is a fundamental parameter for conductive hydrogels. The conductivity of the hydrogels with different compositions was evaluated in Fig. 4a. After introducing DACD to hydrogel system, PGBCDH showed the great ionic conductivity (0.31 S/m), which was higher than PH (0.21 S/m), PGH (0.17 S/m), PBH (0.21 S/m) and PGBH (0.20 S/m). It resulted from that the molecule-ion interaction between DACD and NaCl made the hy-

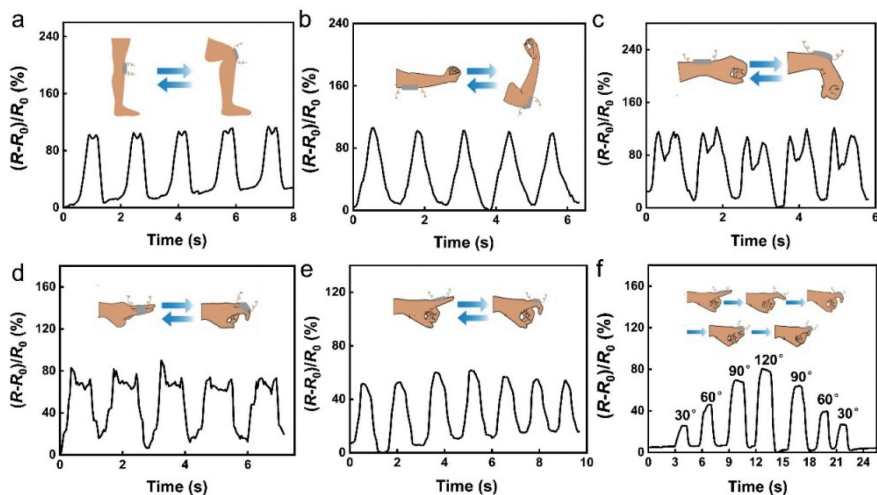


**Fig. 5.** Demonstration of the PGBCDH as flexible wearable sensor for real-time monitoring of big human motions. (a-e) Relative resistance changes for bending and releasing the knee, elbow joint, opisthenar, double and single finger, respectively. (f) Relative resistance changes for bending the index finger at different bending angles (30°, 60°, 90°, and 120°).

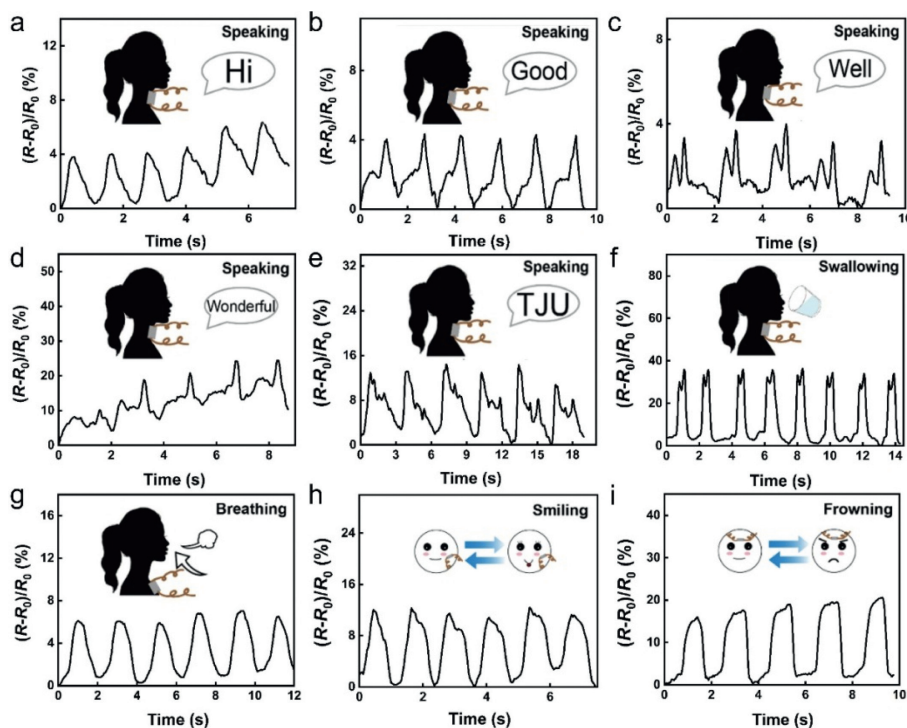


**Fig. 6.** The PGBCDH was attached on the throat as a flexible wearable sensor for real-time monitoring of different voice signals: (a) "Hi"; (b) "Good"; (c) "Well"; (d) "Wonderful"; and (e) "TJU". (f-i) Relative resistance changes when the sensor was attached to the throat, chest, corners of the mouth and forehead to respond small movements, including swallowing, breathing, smiling and frowning, respectively.

drogel exhibit a slight increase in conductivity [30]. When the content of DACD further increased from 0.03% to 0.3% (w/v), the conductivity decreased as the enhanced molecule-ion interaction reduce ionic mobility in solution. To further investigate the potential of PGBCDH as human motion sensors, the conductive stability and strain sensitivity were tested. In Fig. 4b, the relative resistance changes of PGBCDH were all stable under repeated strains of 50%, 100%, 150%, 200% and 250%. The corresponding GFs were 3.98, 4.47, 5.80, 6.27 and 8.57 in 0%–50%, 50%–100%, 100%–150%, 150%–200% and 200%–250% strain, respectively (Fig. 4c). It implied that PGBCDH showed salient sensitivity in the measured strain range. Due to the excellent sensitivity and shape recovery properties, the strain sensor quickly responded within 168 ms for 1000%

$(R - R_0)/R_0$  by instant stretching (Fig. 4d). Furthermore, Fig. 4e showed repeatable  $(R - R_0)/R_0$  in the range of 25–60°C due to good water retention capacity of PGBCDH (Fig. S2 in Supporting information). And the long-term stability of PGBCDH was investigated under cyclic tensile strain of 100% for 200 cycles (Fig. 4f). The result showed that the strain sensing characteristics remained stable over 200 cycles, demonstrating the high reproducibility of ion-conducting PGBCDH as a sensing material with negligible electrical hysteresis and no-decaying  $(R - R_0)/R_0$ .

Due to the excellent mechanical properties, high ionic conductivity, remarkable sensing sensitivity and stability, PGBCDH showed great prospect for use as a wearable sensor. Therefore, the ion-conducting hydrogel-based strain sensor was fabricated and inte-

grated into different parts of the human body to detect complex body movements in real time. When the hydrogel sensor was adhered to the knee, elbow, wrist, double and single finger joints for periodic bending and straightening motions, the  $(R - R_0)/R_0$  changed significantly with respective features and excellent repeatability (Figs. 5a-e). Fig. 5f exhibited the different resistance changes of the index finger at different bending angles from 30° to 120°. It demonstrated the sensor's precise sensing ability for different bending angles. Therefore, PGBCDH can track and distinguish different motion states according to the output of the sensing signal, indicating that the strain sensor has great sensing reliability.

Except for these large movements of body parts, hydrogel sensor can be used to detect subtle changes, like speech recognition capabilities. As shown in Figs. 6a-e, different words can be distinguished by attaching the hydrogel to the throat. The pronunciation of "Hi" showed a characteristic peak, while "Good" and "Well" showed two peaks. And three characteristic signals were observed when saying "Wonderful" and "TJU". These similar characteristic peaks and valleys clearly demonstrated the vocalization identification of PGBCDH sensor when the same phrase was repeated. Therefore, the hydrogel sensor showed the potential applications of voice restoration and articulation rehabilitation. Then, it presented the electrical signals as volunteer swallowed through the regular and stable  $(R - R_0)/R_0$  curve (Fig. 6f). Also, PGBCDH sensor detected normal physiologic deep breathing in a relaxed state and showed distinct and repeatable inspiratory and expiratory output signals (Fig. 6g). As exhibited in Figs. 6h and i, the  $(R - R_0)/R_0$  signals of the facial expression were repetitive and identifiable when volunteer smiled and frowned, respectively. These repeatable output signals indicated the strain sensor had good emotional facial expression recognition ability and high stability. Consequently, PGBCDH can be considered as a promising sensor for omnidirectional detection of human motion as wearable devices.

In summary, the ion-conducting hydrogel (PGBCDH) as flexible wearable sensor was fabricated by the combination of natural Gel-DACD network and synthetic PVA-borax one. Gel-DACD acted as mechanical deformation force through non-covalent cross-linking, endowing PGBCDH with excellent mechanical stress (1.35 MPa), stretchability (400%), toughness (1.84 MJ/m<sup>3</sup>) and excellent fatigue resistance (200% strain for 100 cycles). Surprisingly, PGBCDH displayed good conductivity of 0.31 S/m after introducing DACD to hydrogel network. As a flexible strain sensor, it showed rapid response (168 ms), high strain sensitivity (GF=8.57 in the strain range of 200%–250%) and reliable sensing stability (100% strain for 200 cycles). PGBCDH-based sensor can accurately monitor complex body movements (knee, elbow, wrist and finger joints) and large-scale subtle movements (speech, swallow, respiration and facial expressions). In sum, it can be considered as one of the potential

candidates for flexible electronic skins for human monitoring with stability and high-accuracy.

### Declaration of competing interest

The authors declare no competing financial interest to influence the work reported in this paper.

### Acknowledgments

This work was supported by National Key R&D Program of China (Nos. 2019YFC1905500 and 2021ZD0201604), National Natural Science Foundation of China (Nos. U20A20261, 31870948, 31971250 and 21922409), Seed Foundation of Tianjin University (No. 2022XXY-0009).

### Supplementary materials

Supplementary material associated with this article can be found, in the online version, at doi:10.1016/j.ccl.2022.107892.

### References

- [1] Y. Ohm, C. Pan, M.J. Ford, et al., *Nat. Electron.* 4 (2021) 185–192.
- [2] Y. Ma, Y. Zhang, S. Cai, et al., *Adv. Mater.* 32 (2020) 1902062.
- [3] Q. Zhong, B. Liu, B. Yang, et al., *Chin. Chem. Lett.* 32 (2021) 3496–3500.
- [4] L. Yao, T. Cheng, X. Shen, et al., *Chin. Chem. Lett.* 29 (2018) 587–591.
- [5] G. Su, S. Yin, Y. Guo, et al., *Mater. Horiz.* 8 (2021) 1795–1804.
- [6] H. Sun, Y. Zhao, C. Wang, et al., *Nano Energy* 76 (2020) 105035.
- [7] A.I. Robby, S.G. Kim, H.J. Jo, et al., *Appl. Mater. Today* 25 (2021) 101259.
- [8] W. Yuan, X. Qu, Y. Lu, et al., *Chin. Chem. Lett.* 32 (2021) 2021–2026.
- [9] S. Liu, X. Tian, X. Zhang, et al., *Chin. Chem. Lett.* 33 (2022) 2205–2211.
- [10] Z. Zhang, L. Tang, C. Chen, et al., *J. Mater. Chem. A* 9 (2021) 875–883.
- [11] M. Liao, P. Wan, J. Wen, et al., *Adv. Funct. Mater.* 27 (2017) 1703852.
- [12] M.A. Darabi, A. Khosrozadeh, R. Mbeleck, et al., *Adv. Mater.* 29 (2017) 1700533.
- [13] Y. Jian, S. Handschuh-Wang, J. Zhang, et al., *Mater. Horiz.* 8 (2021) 351–369.
- [14] Y. Niu, H. Liu, R. He, et al., *Mater. Today* 41 (2020) 219–242.
- [15] Y. Wang, M. Tebyetekerwa, Y. Liu, et al., *Chem. Eng. J.* 420 (2021) 127637.
- [16] J. Wen, J. Tang, H. Ning, et al., *Adv. Funct. Mater.* 31 (2021) 2011176.
- [17] R. Tong, G. Chen, D. Pan, et al., *Biomacromolecules* 20 (2019) 2096–2104.
- [18] J.P. Gong, Y. Katsuyama, T. Kurokawa, Y. Osada, *Adv. Mater.* 15 (2003) 1155–1158.
- [19] Q. Chen, H. Chen, L. Zhu, J. Zheng, *J. Mater. Chem. B* 3 (2015) 3654–3676.
- [20] J.Y. Sun, X. Zhao, W.R. Illeperuma, et al., *Nature* 489 (2012) 133–136.
- [21] B. Yang, W. Yuan, *ACS Appl. Mater. Interfaces* 11 (2019) 16765–16775.
- [22] H. Ding, X. Liang, Q. Wang, et al., *Carbohydr. Polym.* 248 (2020) 116797.
- [23] Z. Qin, D. Dong, M. Yao, et al., *ACS Appl. Mater. Interfaces* 11 (2019) 21184–21193.
- [24] Z. Qin, X. Sun, H. Zhang, et al., *J. Mater. Chem. A* 8 (2020) 4447–4456.
- [25] A. Roy, K. Manna, P.G. Ray, S. Dhara, S. Pal, *ACS Appl. Mater. Interfaces* 14 (2022) 17065–17080.
- [26] X. Liu, Z. Ren, F. Liu, et al., *ACS Appl. Mater. Interfaces* 13 (2021) 14612–14622.
- [27] M. Liao, H. Liao, J. Ye, P. Wan, L. Zhang, *ACS Appl. Mater. Interfaces* 11 (2019) 47358–47364.
- [28] Y. Ma, Y. Gao, L. Liu, X. Ren, G. Gao, *Chem. Mater.* 32 (2020) 8938–8946.
- [29] L. Wang, H.J. Zhang, X. Liu, et al., *ACS Appl. Polym. Mater.* 3 (2021) 3197–3205.
- [30] L.X. Song, S.Z. Pan, L. Bai, et al., *Supramol. Chem.* 23 (2011) 447–454.